Light Metals 2011 *Edited by: Stephen J. Lindsay*
TMS (The Minerals, Metals & Materials Society), 2011

THE COUPLING OF MACROSEGREGATION WITH GRAIN NUCLEATION, GROWTH AND MOTION IN DC CAST ALUMINUM ALLOY INGOTS

Miha Založnik[1], Arvind Kumar[1], Hervé Combeau[1], Marie Bedel[1,2], Philippe Jarry[2], Emmanuel Waz[2]

[1]Institut Jean Lamour, CNRS – Nancy-Université – UPV-Metz,
Ecole des Mines de Nancy, Parc de Saurupt CS 14234, F-54042 Nancy cedex, France
[2]Alcan CRV, 725 Rue Aristide Bergès, BP 27, F-38341 Voreppe cedex, France

Keywords: Direct chill casting, Aluminum alloys, Solidification, Macrosegregation, Microstructure

Abstract

The phenomena responsible for the formation of macrosegregations, and grain structures during solidification are closely intertwined. We present a model study of the formation of macrosegregation and grain structure in an industrial sized (350 mm thick) direct chill (DC) cast aluminum alloy slab. The modeling of these phenomena in DC casting is a challenging problem mainly due to the size of the products, the variety of the phenomena to be accounted for, and the non-linearities involved. We used a volume-averaged multiscale model that describes nucleation on grain refiner particles and grain growth, coupled with macroscopic transport: fluid flow driven by natural convection and shrinkage, transport of free-floating globular equiaxed grains, heat transfer, and solute transport. We analyze the heat and mass transfer in the slurry moving-grain zone that is a result of the coupling of the fluid flow and of the grain nucleation, growth and motion. We discuss the impact of the flow structure in the slurry zone and of the grain packing fraction on the macrosegregation.

Introduction

The macrosegregation in the DC casting process is governed mainly by two mechanisms: by the melt flow induced by thermosolutal natural convection, shrinkage and pouring, and by the transport of solute-lean free-floating grains [1–6]. A commonly observed, surface-to-surface distribution of alloying elements at a transverse cross-section of a DC cast ingot reveals distinct regions of positive (solute-rich) and negative (solute-depleted) segregation [1]. A solute-depleted region is present in the ingot center, adjoined by a positive segregation zone spreading into the outward direction, an adjacent thin negative segregation zone and another positive segregation layer at the surface. Experimental investigations were published on macrosegregation and macrostructure in grain refined and non-grain refined ingots [2,7]. It was reported that macrosegregation generally increases with grain refinement and linked this to the increased transport of free-floating coarse (slowly growing) grains, formed either by the fragmentation of dendrites or by nucleation on grain refiner particles. Eskin et al. [7] presented a systematic experimental investigation of the dependence of macrosegregation and structure on process parameters. A strongly supported hypothesis states that the negative centerline segregation is caused by the transport of solute-lean free-floating grains to the center of the casting.

First attempts to model the influence of free-floating grains were made by Reddy and Beckerman [3]. They considered nucleation of grains at a fixed temperature and the transport and growth of spherical globular grains in a slurry zone. The solid phase was assumed to form a connected rigid porous structure (packing) at a solid volume fraction of 0.637 (packing fraction). In the case of simulations accounting for grain motion, a significant negative segregation at the center of the billet was found. Vreeman et al. [4,5] proposed a simplified model with regard to grain nucleation and growth, assuming local equilibrium (lever rule) and a constant imposed characteristic grain diameter. They calculated the grain velocity directly from the grain diameter and the solid fraction. Macrosegregation distributions in DC cast billets were calculated [5] and a parametric study of two key model parameters, the packing fraction and the grain diameter, was performed for Al-4.5 wt%Cu and Al-6 wt%Mg billets with a diameter of 400 mm. The results were qualitatively consistent with commonly observed macrosegregation trends. The study revealed a large degree of dependence on both the packing fraction and grain diameter. It has to be noted that their imposed grain diameter has to represent an actual grain size distribution and that the packing fraction is not well known and, moreover, might not be uniform throughout the mushy zone. In a later work Vreeman et al. [4] compared model predictions to measurements on industrial-scale 450 mm diameter DC cast billets of an Al-6 wt%Cu alloy and tried to determine the value of the packing fraction to obtain the best fit. They found rea-

sonably good agreement between the experimental and model results and they estimated the packing fraction to be in the range of 0.2–0.3. For a more detailed overview of macrosegregation modeling the reader is directed to the recent extensive review [1].

We recently conducted a systematic study of the influence of the individual transport mechanisms, viz. shrinkage, natural convection and grain motion, and their interactions, on the macrosegregation formation [10]. In the present paper we go further and analyze in more detail the heat and mass transfer in the slurry moving-grain zone that is a result of the coupling of the fluid flow and the grain nucleation, growth and motion. We discuss the impact of the flow structure in the slurry zone and of the grain packing fraction on the grain growth, motion and the resulting macrosegregation.

Model

Physical Model and Solution Procedure

The multiscale two-phase model SOLID is presented in entirety in [8]. We here therefore provide only a brief description and point out model extensions with respect to ref. [8]: the consideration of nucleation on inoculant particles and their transport, and the consideration of shrinkage-induced fluid flow in the mushy zone. The model is based on a volume-averaged Euler-Euler two-phase model that consists of two parts: a macroscopic part with momentum, mass, heat, solute mass, and grain population conservation equations, and a microscopic part that describes the nucleation and growth of grains. At the macroscopic level, the model accounts for heat and solute transport coupled with flow driven by thermal and solutal buoyancy and by solidification shrinkage (assuming no strain in the solid). Depending on the behavior of the solid phase, we consider two flow regimes in the mushy zone. Where the solid volume fraction g_s is larger than the packing limit ($g_s > g_s^{pack}$) the solid is considered to be blocked and moving at the casting velocity. The flow of intergranular liquid through the porous solid matrix is described by a momentum equation including a Darcy term for the drag interactions, with the permeability modeled by the Kozeny-Carman law. The density of the solid phase is assumed to be constant and for the liquid density the Boussinesq assumption is employed. The flow due to solidification shrinkage is induced via the enforcement of mass conservation, by considering different densities of the solid and liquid phases. At solid fractions smaller than the packing limit ($g_s < g_s^{pack}$) the solid phase is considered to be in the form of free-floating grains. Their motion is described by a balance of buoyancy, drag and pressure forces acting on a grain. In this way, the solid and liquid have locally different velocities. The interfacial particle drag is considered dependent on the grain size, which produces the tendency that the larger the grains are, the stronger their tendency to settle; contrarily, smaller grains are more easily entrained by the liquid motion.

The microscopic level is treated locally; within SOLID, this means within each discrete volume element. The nucleation is controlled by the addition of inoculants. According to the theory of Greer et al. [9] an inoculant particle is activated as a nucleation (or better, growth-onset) site at a critical undercooling that is inversely proportional to its size: $\Delta T_{uc}(d) \propto d^{-1}$. A typical particle size distribution in the active particle range in a commercial inoculant is exponential. The largest particles nucleate first and afterwards a nucleation-growth competition takes place. As long as the number of nucleated grains is still small, the solidification kinetics is too slow and the constitutional undercooling will continue to increase, triggering the nucleation on smaller particles. As the grain density increases, the growth kinetics of the nucleated grains approaches equilibrium and the undercooling decreases; further nucleation is blocked. This physics is modeled by considering a distribution of inoculant particle size, discretized into 10 classes. Each class has its own activation undercooling, depending on the mean particle size in the class, and an initial density, calculated from the known distribution density. Moreover, the transport of nuclei is considered, assuming that they move at the velocity of the liquid. The conservation equation for nuclei of class i is

$$\frac{\partial N_{nucl}^{i}}{\partial t} + \nabla \cdot \left(\vec{v}_l N_{nucl}^{i}\right) = \Phi^{i} \tag{1}$$

$$\Phi^{i} = \begin{cases} -N_{nucl}^{i}\delta(t) & \text{if } \Delta T_{uc} < \Delta T_{nucl}^{i} \\ 0 & \text{else} \end{cases} \tag{2}$$

where N_{nucl}^{i} is the volume density of nuclei of class i, $\vec{v}_l$ is the intrinsic velocity of the liquid, Φ^{i} is the nucleation source term, δ is the Dirac delta function, $\Delta T_{uc} = m_L(C_l^* - C_l)$ is the local undercooling, m_L is the liquidus slope, C_l^* is the concentration of liquid at the solid-liquid interface, C_l is the local average concentration of the liquid, and ΔT_{nucl}^{i} is the activation undercooling for the nuclei particles of class i. At the same time the conservation equation for grains is

$$\frac{\partial N}{\partial t} + \nabla \cdot (\vec{v}_s N) = -\sum\nolimits_i \Phi^{i} \tag{3}$$

where N is the local volume density of grains and $\vec{v}_s$ is the velocity of the solid grains. The source term accounts for nucleation of grains from the grain refiner particles. The nucleation is solved coupled with the macroscopic transport and the likewise local (microscopic) phase-change. The phase change (solidification and melting) is controlled by solute diffusion in both phases at the grain scale, assuming local thermal equilibrium and thermodynamic equilibrium at the solid-liquid interface. In the present work the grains are considered spherical with a fully globular morphology, which in many cases can be considered as a realistic assumption for inoculated DC cast aluminum alloys.

We solve the macroscopic equations with a finite-volume method. The local microscopic growth model is integrated implicitly and is coupled with the microscopic nucleation and the macroscopic model via a three-step operator-splitting integration method that separates the integration of the macroscopic terms and the microscopic nucleation and growth terms into three separate stages. This method is an extension of the algorithm [8] that introduces a separate solution step for the nucleation.

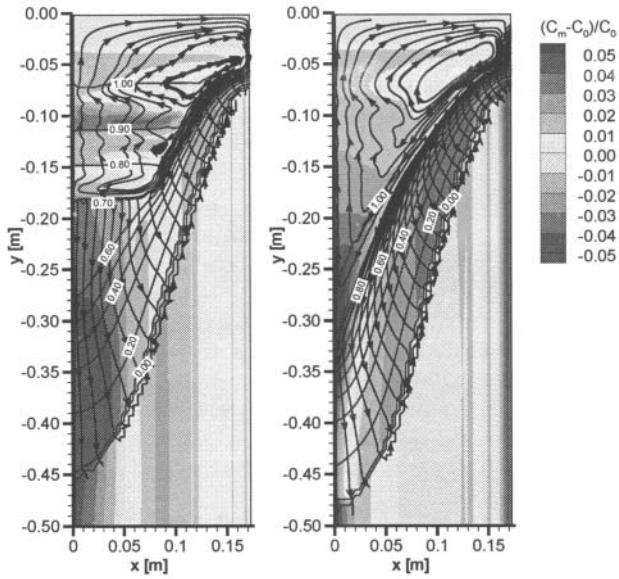

Figure 1: Segregation and streamlines of relative liquid velocity ($\vec{v}_l - \vec{v}_{cast}$). Left: $g_s^{pack} = 0.3$. Center: $g_s^{pack} = 0$.

Process Model

We studied the solidification in a 7449 alloy slab of 350 mm thickness. We consider a simplified 2D geometry with symmetry, i.e. a domain of 175×800 mm. The computational grid consists of 40×115 rectangular cells, refined in the solidifying and liquid zones. The solidified metal leaves the domain at a casting speed of 75 mm/min at the bottom. Note that this casting speed is much higher than the industrial practice, which we did to amplify the macrosegregation. The feeding of the liquid metal with the nominal composition, inoculant particle density distribution and casting temperature is at the top across the whole cross section. The feeding velocity is uniform across the inlet and is given by a mass balance accounting for the solidification shrinkage. The heat extraction in the mold is described by three zones with different heat transfer coefficients: a meniscus at the top, a contact zone, and an air-gap zone. The heat extraction in the water-chill under the mold is described by the classical Weckman-Niessen correlation.

The 7449 alloy was modeled in a simplified way, as an equivalent pseudo binary alloy, the approximation done to match the solidification path of the multicomponent 7449 alloy, calculated with a Calphad model. This gave a partition coefficient of 0.257, a linear liquidus slope of -6.05 K/wt%, and a melting temperature of pure Al at 677.8 °C (a projection of the liquidus to $C = 0$). The alloy is further modeled with constant density of the solid and a Boussinesq approximation with constant thermal and solutal expansion coefficients for the liquid. The liquid density is thus variable in the buoyancy terms, for both the liquid and the solid force balance (the grain buoyancy depends on $(\rho_s - \rho_l)$), but is constant in the mass balance. The shrinkage coefficient $\beta_{sl} = (\rho_s/\rho_{l,ref} - 1)$ is thus constant; we used $\beta_{sl} = 0.057$. The thermal and solutal expansion coefficients were modeled to fit the variation of liquid density along the solidification path of the 7449 alloy. For this alloy thermal and solutal expansion are cooperating and the influence of heavier solutes rejected into the liquid upon solidification dominates.

Results and Discussion

The Role of Grain Motion in Segregation Formation

When a part of the grains growing in the mushy zone of a DC cast ingot are free to move, these grains, as they are usually heavier than the surrounding liquid, have a tendency to settle. They settle along the inclined mushy zone towards the center, where they accumulate at the bottom of the sump. Upon settling of the solute-lean grains the solute-rich liquid is expelled upwards and this creates a negative macrosegregation tendency in the center of the ingot (Fig. 1). In addition to the grains, the

liquid is also set in motion. In the slurry zone the principal driving force for fluid motion is the entrainment by the moving grains; additionally, thermal and solutal buoyancy forces can induce motion too. This flow is globally downwards with the fast current of settling grains along the packing front, and recirculating slowly back upwards in the center (Figs. 1 and 4). The upward flow entrains some grains, which creates the extended slurry zone. Just below the packing front the thermosolutal buoyancy is the prime driving force for the intergranular fluid flow through the packed porous solid matrix. A little deeper into the mushy zone at smaller liquid fractions the permeability strongly decreases, so the high flow resistance completely blocks the natural convection flow. The flow is now controlled by the solidification shrinkage that creates a high pressure drop and orients the flow towards the solidification front (Fig. 1).

Corresponding to this flow situation we can distinguish four zones for segregation formation: the slurry zone, the packing front, the moderately permeable packed layer (moderate g_l), and the impermeable packed layer (low g_l). We investigated these interactions in [10], where we have shown that the grain transport is not only directly responsible for the creation of the negative centerline segregation, but also changes the sump shape and thus modifies the action of the natural convection and shrinkage flow and the segregaton they cause. While it is generally supported that the transport of solute-lean free-floating grains causes a negative segregation at the centerline, where they settle, the modification that comes with the intensity of grain transport is not clear a-priori. We would expect that as more grains are free to move and settle, the negative centerline segregation will be amplified. A numerical parameter study of the dependence of the centerline segregation on the packing fraction (g_s^{pack}) shows a quite nonlinear image (Fig. 2). We can see that the centerline segregation in a columnar ingot is strongly positive (Figs. 1, 2). When a part of the grains is free to move the centerline segregation drops sharply at low g_s^{pack} and quickly reaches a negative centerline segregation (at $g_s^{pack} \sim 0.05$). As the proportion of free grains increases, the centerline segregation continues to drop, until it reaches a minimum (at $g_s^{pack} \sim 0.25$ in our example) and then increases again for higher g_s^{pack}.

Let us look in more detail at what happens in Fig. 2. As the packing fraction is increased, more grains are free to settle at the bottom. At low packing fractions the impact of the solute transport by solute-lean grains remains relatively fable. The grain transport by itself does not provoke the sharp decrease of the positive centerline segregation. However, the segregation caused in the low-solid-

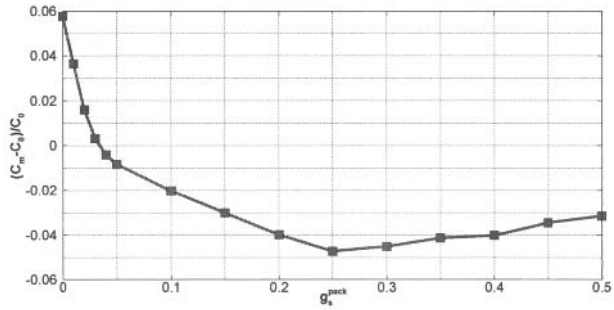

Figure 2: Dependence of the centerline segregation on the packing fraction.

fraction region of the mushy zone is reduced due to a lower velocity difference $\vec{v}_s - \vec{v}_l$ (the grains move). In the packed region, on the other hand, the segregation is weaker than before since the liquid flow is less intense due to a lower permeability of the packed region. As the packing fraction is increased further, this effect becomes stronger and stronger. At the same time the solute transport by grain settling starts to become important. We now find a negative segregation in the center (at $g_s^{pack} \sim 0.05$). From this point on, a large slurry zone develops with a particular flow structure (Fig. 4), where the flow descends in a strong current limited to the close vicinity of the packing front and the liquid ascends slowly in the almost stagnant core of the slurry zone. The grains that are carried into the core settle downwards very slowly in a countercurrent motion, some are even entrained by the liquid and leave and remelt into the fully liquid zone.

How is this flow set up? We can observe that the liquid in the core of the slurry zone is close to thermodynamic equilibrium. As we will see later, this happens because of the slow phase change (solidification/melting) of the floating grains. The slow phase change means that the solute exchange of the interface of a grain is slow and the diffusion in the liquid surrounding a grain has enough time to maintain the liquid close to the thermodynamic equilibrium concentration at the interface. This means that the temperature and the liquid concentration are closely coupled, which can be described by the equilibrium relation $T = T_f + m_L C_l$ for the liquidus temperature. As the solutal effect on the buoyancy force is much stronger than the thermal one, and the Schmidt number $Sc = D/\nu \sim 100$ of the solution is very high, the dominating solutal buoyancy creates a stable solutal stratification. The coupling of the temperature and the concentration maintained by the phase change then induces a corresponding thermal stratification, stable as well (Fig. 4). The solid fraction is

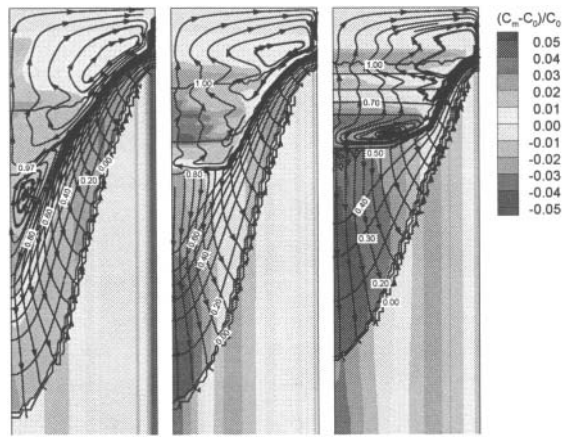

Figure 3: Segregation and streamlines ($\vec{v}_\mathrm{l} - \vec{v}_\mathrm{cast}$) for different packing fractions. Left: $g_\mathrm{s}^\mathrm{pack} = 0.03$. Center: $g_\mathrm{s}^\mathrm{pack} = 0.20$. Right: $g_\mathrm{s}^\mathrm{pack} = 0.50$.

stably stratified too. In this situation the driving force for the flow comes from the lateral gradients of temperature, concentration and, most notably, solid fraction, which are localized next to the inclined packing front in the growth region and drive the descending current.

The relative grain settling velocity $\vec{v}_\mathrm{s} - \vec{v}_\mathrm{l}$ is essentially driven by a balance of buoyancy and drag forces acting on the grains. If we simplify this force balance, we can show that essentially, the settling velocity of a globular grain is proportional to the density difference between solid and liquid and the square of the grain size: $\vec{v}_\mathrm{s} - \vec{v}_\mathrm{l} \propto (\rho_\mathrm{s} - \rho_\mathrm{l}) d^2$. While the grain size can differ and is dependent on a rather complex nucleation-growth competition in the nucleation zone as well as the grain transport, we did not observe a fundamental variation with grain size as a function of the packing fraction. The decisive factor is the density difference ($\rho_\mathrm{s} - \rho_\mathrm{l}$). The density of the liquid phase depends on its temperature and composition. In the present case, where the alloying elements are heavier than aluminum, the density of the liquid increases as solidification progresses. This can be demonstrated by applying a Scheil solidification path to the density function $\rho_\mathrm{l} = \rho_{\mathrm{l,ref}}(1 - \beta_T(T - T_\mathrm{ref}) - \beta_C(C_\mathrm{l} - C_\mathrm{ref}))$. The density of the primary solid phase, on the other hand, is approximately constant. At the onset of solidification the solid density is greater, however in many alloys the liquid density becomes larger at a certain solid fraction. In the modeled alloy this happens at approximately $g_\mathrm{s} = 0.30$. The grain settling velocity slows down and even reverses

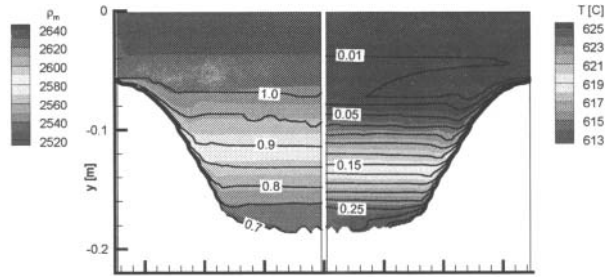

(a) Stratification controlling the flow in the slurry zone. Left: average density ρ_m (color map) and liquid fraction. Right: temperature (color map) and liquid concentration (contour lines in mass fraction).

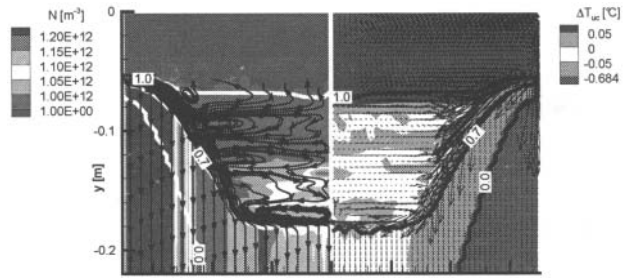

(b) Grain nucleation, growth, motion and accumulation. Left: grain population density and solid velocity streamlines (an approximation for the grain trajectories due to a qualitatively steady state). Right: undercooling ($-0.684\,^\circ$C is the activation undercooling for the largest inoculant particles) and liquid velocity vectors. The liquidus, packing ($g_\mathrm{s}^\mathrm{pack} = 0.3$) and solidus fronts are marked.

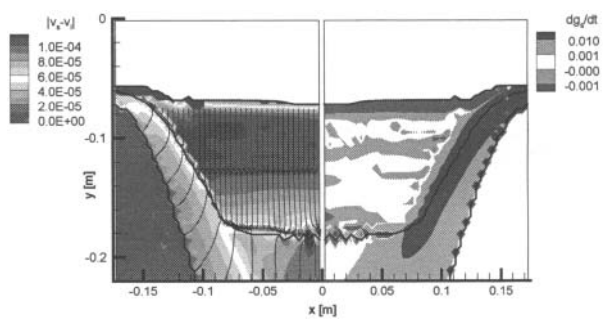

(c) Grain motion and growth. Left: relative grain velocity ($\vec{v}_\mathrm{s} - \vec{v}_\mathrm{l}$)) magnitude and streamlines. Right: solidification rate ($\partial g_\mathrm{s}/\partial t > 0$ for solidification and $\partial g_\mathrm{s}/\partial t < 0$ for melting).

Figure 4: Flow, motion, nucleation, growth and coalescence of free-floating grains – conditions in the slurry zone for $g_\mathrm{s}^\mathrm{pack} = 0.3$.

(i.e. the grains start to float upwards) for high packing fractions, $g_\mathrm{s}^\mathrm{pack} > 0.30$ (Figs. 3 and 4). The decreased grain transport reduces the negative centerline segregation. At the same time the shape of the sump is modi-

fied as more grains settle to the center with an increasing g_s^{pack}. The packed part of the mushy zone becomes shallower and the streamlines of the shrinkage-induced flow in this region are less divergent. The shrinkage induced segregation in the center is thus reduced.

Grain Nucleation, Growth and Motion in the Slurry Zone

The flow enters the slurry zone exclusively in the stream flowing downward along the packing front. This is shown in Fig. 4. Analyzing the grain trajectories we can see that the grains then either attach to the front, settle to the bottom of the slurry zone or enter the core of the slurry zone. In the core the grains slowly settle downwards before rejoining the stream and settling to the bottom of the sump. The residence time of these latter grains in the core is rather long and they have enough time to regain equilibrium. We can see in Fig. 4 that the core is a zone of very small undercoolings/superheats and the phase change rate is correspondingly small. This is a zone of very slow growth and partial remelting of the free-floating grains, which is also shown in Fig. 4. The undercoolings ΔT_{uc} in the core are also not enough to trigger nucleation in this zone. This means that the grains here all originated elsewhere and were transported here. The zone of higher undercoolings is located along the packing front in the main stream (Fig. 4). This is the region of nucleation and fast growth. The free floating-grains thus nucleate mainly in the stream entering the slurry zone. They first grow fast while descending along the packing front and then their growth slows down as they float around in the stagnant slurry zone.

Conclusions

We analyzed the coupling of the flow structure in the slurry zone, grain growth and motion, and macrosegregation. The grain settling dynamics strongly depends on the packing fraction and is closely coupled with the segregation. We could show that the grains initially nucleate and grow fast in a zone of high undercooling, while settling along the packing front. They then continue with a phase of slow growth while floating in the core of the slurry zone.

Acknowledgements

This work was supported by Alcan CRV.

References

[1] R. Nadella et al., "Macrosegregation in direct-chill casting of aluminium alloys," *Prog. Mater. Sci.*, 53 (2008), 421–480.

[2] G. Lesoult et al., "Equi-axed growth and related segregations in cast metallic alloys," *Sci. Technol. Adv. Mat.*, 2 (2001), 285–291.

[3] A. V. Reddy and C. Beckermann, "Modeling of macrosegregation due to thermosolutal convection and contraction-driven flow in direct chill continuous casting of an Al-Cu round ingot," *Metall. Mater. Trans. B*, 28B (1997), 479–489.

[4] C. J. Vreeman, J. D. Schloz, and M. J. M. Krane, "Direct chill casting of aluminum alloys: Modeling and experiments on industrial scale ingots," *J. Heat Trans.-T. ASME*, 124 (2002), 947–953.

[5] C. J. Vreeman and F. P. Incropera, "The effect of free-floating dendrites and convection on macrosegregation in direct chill cast aluminum alloys, part II: Predictions for Al-Cu and Al-Mg alloys," *Int. J. Heat Mass Tran.*, 43 (2000), 687–704.

[6] M. Založnik and B. Šarler, "Modeling of macrosegregation in DC casting of aluminum alloys: Estimating the influence of casting parameters," *Mater. Sci. Eng. A*, 413-414 (2005), 85–91.

[7] D. G. Eskin et al., "Structure formation and macrosegregation under different process conditions during DC casting," *Mater. Sci. Eng. A*, 384 (2004), 232–244.

[8] M. Založnik and H. Combeau, "An operator splitting scheme for coupling macroscopic transport and grain growth in a two-phase multiscale solidification model: Part I – model and solution scheme," *Comp. Mater. Sci.*, 48 (2010), 1–10.

[9] A. L. Greer et al., "Modelling of inoculation of metallic melts: Application to grain refinement of aluminium by Al-Ti-B," *Acta Mater.*, 48 (2000), 2823–2835.

[10] M. Založnik et al., "Influence of transport mechanisms on macrosegregation formation in direct chill cast industrial scale aluminum alloy ingots," *Matériaux 2010*, submitted to *Adv. Eng. Mater.* (2010).